AIP | Applied Physics Letters

Room temperature photocurrent spectroscopy of single zincblende and wurtzite InP nanowires

A. Maharjan, K. Pemasiri, P. Kumar, A. Wade, L. M. Smith, H. E. Jackson, J. M. Yarrison-Rice, A. Kogan, S. Paiman, Q. Gao, H. H. Tan, and C. Jagadish

Citation: Applied Physics Letters **94**, 193115 (2009); doi: 10.1063/1.3138137
View online: http://dx.doi.org/10.1063/1.3138137
View Table of Contents: http://scitation.aip.org/content/aip/journal/apl/94/19?ver=pdfcov
Published by the AIP Publishing

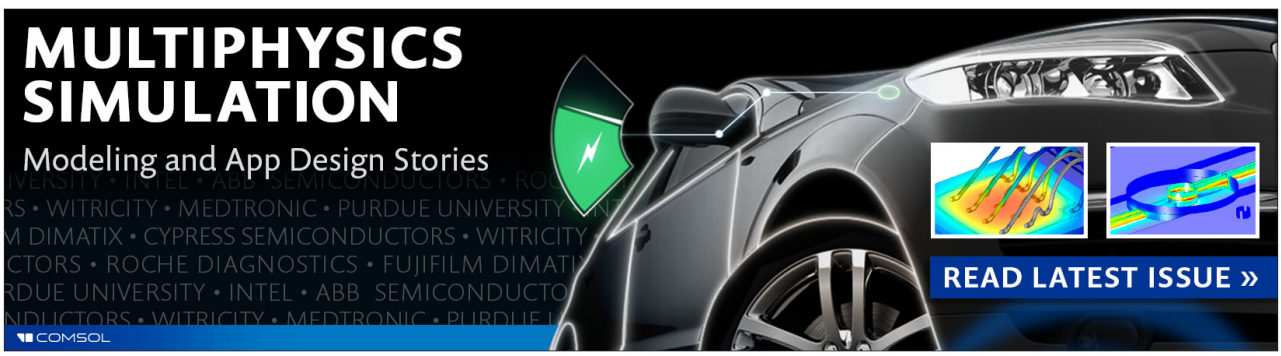

Room temperature photocurrent spectroscopy of single zincblende and wurtzite InP nanowires

A. Maharjan,[1] K. Pemasiri,[1] P. Kumar,[1] A. Wade,[1] L. M. Smith,[1,a)] H. E. Jackson,[1] J. M. Yarrison-Rice,[2] A. Kogan,[1] S. Paiman,[3] Q. Gao,[3] H. H. Tan,[3] and C. Jagadish[3]
[1]*Department of Physics, University of Cincinnati, Cincinnati, Ohio 45221-0011, USA*
[2]*Department of Physics, Miami University, Oxford, Ohio 45056, USA*
[3]*Department of Electronic Materials Engineering, Research School of Physics and Engineering, Australian National University, Canberra, Australian Capital Territory 0200, Australia*

(Received 14 April 2009; accepted 24 April 2009; published online 15 May 2009)

Simple photolithographic techniques are used to fabricate single InP nanowire devices with back-to-back Schottky barriers. Direct imaging of the photoresponse shows that the active regions of the device are spatially localized near the reverse-biased Schottky barrier. By tuning the laser excitation energy from below to well above the energy gap, photocurrent spectroscopy can illuminate the zincblende or wurtzite nature of the nanowire device even at room temperature. © *2009 American Institute of Physics*. [DOI: 10.1063/1.3138137]

The synthesis and electronic characterization of semiconductor nanowires have received significant recent attention as a possible route toward room-temperature electronics utilizing quantum effects.[1] While the properties of a nanostructured material can be significantly changed because of quantum effects, here we study a distinctively different example, namely, that of a change in the crystalline structure of the InP nanowire (NW). InP is a direct band gap material used in high power and high frequency applications because of its excellent transport properties. While bulk InP only exists as a cubic zincblende (ZB) structure, InP nanowires have recently been synthesized with the cubic ZB structure and with the hexagonal wurtzite (WZ) structure, as well as mixed ZB/WZ homostructures.[2–4] In addition, time-resolved photoluminescence measurements in a ZB/WZ mixed structure have shown that both the electrons and the holes can be significantly quantum confined to the ZB or WZ layers in a type II structure.[4] Such structures may lead to interesting device architectures as controlled growth of WZ or ZB structures are beginning to be achieved.[5,6]

Previously, Tragardh *et al.*[7] used photocurrent spectroscopy to determine the band gap of short InAsP sections embedded inside InAs nanowires. The measurements were performed at low temperatures and required Ohmic contacts to be fabricated using e-beam lithography and liftoff on the InAs end segments. In this paper, we demonstrate that by using simple photolithographic techniques, one can rapidly fabricate a metal-semiconductor-metal (MSM) nanodevice which is sensitive to the photon energy near the band gap at room temperature. Dark current measurements indicate that the device is operating as back-to-back Schottky barriers, while spatially-resolved photocurrent measurements display the largest response near the reverse-biased Schottky barrier. Detailed measurements of the photocurrent response as a function of laser excitation in a single nanowire device at room temperature sensitively determine that the band gap of InP WZ nanowires is 1.408 eV, ~70 meV larger than that of ZB nanowires, in agreement with a number of recent low temperature optical measurements.[3,4,7,8]

The InP nanowires are grown by vapor-liquid-solid growth catalyzed by 20 and 50 nm gold nanoparticles on an InP substrate at 400 C using metal-organic chemical-vapor deposition. The 50 nm nanowires were grown with a V/III ratio of 350, while the 20 nm nanowires were grown at a V/III ratio of 700.[9] Extensive cw and time-resolved PL measurements at low temperatures have shown that the 20 nm wires are predominantly WZ, while the 50 nm nanowires are predominantly ZB, with some twins and stacking faults present as determined by high-resolution transmission electron microscopy imaging.[3,4,9] To obtain individual nanowires, the growth substrate was sonicated in a methanol solution and then dispersed onto a Si substrate capped with a thermally grown 400 nm SiO_2 insulating layer. A standard photoresist layer is spun onto the Si substrate. To fabricate a device, a photomask was designed which consists of two large 200 μm windows (which become the contact pads for later wire bonding) with small micron-sized protrusions which form a 1–5 μm gap to form the actual nanowire contacts. Since the nanowires here are ~6 μm long, this procedure allows us to easily image the nanowires through the large windows and then position the protrusions over the ends of the nanowire for UV exposure. After development, standard deposition and liftoff techniques were used to fabricate the Ti/Al contact pads across the nanowire separated by a ~3 μm gap; this then results in an MSM arrangement. We used a CW Ti-sapphire laser tuned from 700 to 1000 nm, mechanically chopped at 280 Hz, to induce a photocurrent. The photocurrent detection circuit consisted of a current amplifier and digital lock-in amplifier. In experiments with diffuse laser illumination, the laser (~25 μW) was partially focused with a 10× objective so as to uniformly illuminate the entire NW device. To obtain spatially resolved photocurrent maps, we focused a 514 nm argon ion laser to an ~0.8 μm spot using a 0.75 numerical aperture ultralong working distance 100× objective, and raster-scanned the sample underneath the objective by using x-y piezoelectric translators capable of nanometer resolution.

Figure 1 shows the *I-V* characteristics of a ZB (50 nm in diameter) device in the dark (red curve) and under 820 nm laser illumination (blue curve) with a power density of

a)Electronic mail: leigh.smith@uc.edu.

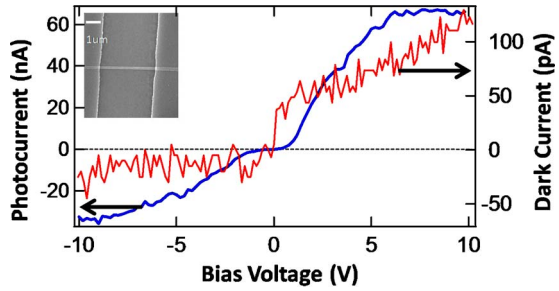

FIG. 1. (Color online) Dark current (red curve; right axis) and photocurrent (blue curve; left axis) for a ZB nanowire device are shown as function of the voltage applied between the metal terminals. The photocurrent exceeds the dark current by nearly three orders of magnitude for a bias of 5 V and excitation at a wavelength of 820 nm and a power density of 30 W/cm^2. Inset: a SEM image of a MSM device used in the measurements. The scale bar is 1 μm.

30 W/cm^2. The dark current in an MSM device is limited by the tunneling of electrons across the Schottky barrier at the reversed bias contact, which results in a nonlinear *I-V* curve.[10] Assymmetry of the observed dark *I-V* curve indicates that the Schottky diodes on each end of the NW are not identical. As can be seen on the plot, illuminating the moderately biased device with the laser tuned above the band gap increases the current by a factor of 1000 or more (blue curve).

An image of the photocurrent as a function of position of the ~0.8 μm laser spot (8 nW incident power or 2 W/cm^2) shows that a large photocurrent appears when the wire is illuminated near the reverse-biased contact, as can be seen in Fig. 2. A similar effect was reported in CdS nanowire MSM devices[11,12] and attributed to the difference in the electron and hole mobilities. We note that the depletion width in our

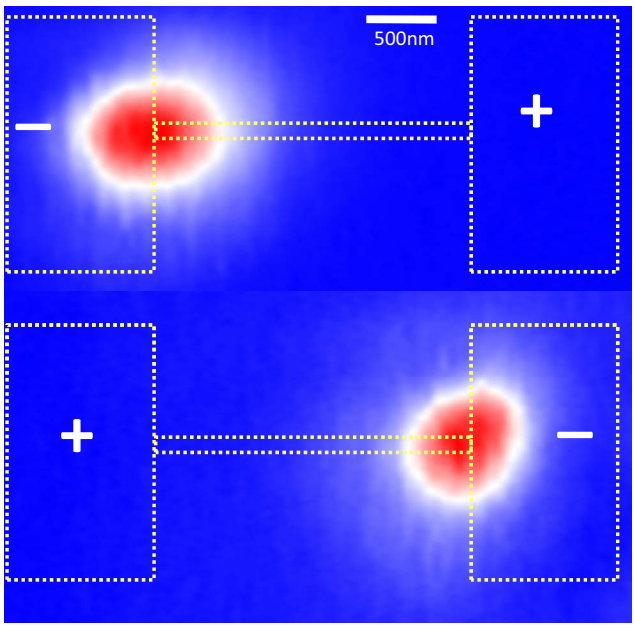

FIG. 2. (Color online) A 2D map of the photocurrent for the same NW obtained by scanning the laser spot over the device region with both positive and negative 5 V bias and a laser power density of 2 W/cm^2 at 514 nm (8 nW incident power). The largest response, a photocurrent of 2 nA, is observed when the laser illuminates the contact injecting electrons into the nanowire, specifically at the reverse-biased Schottky barrier. The dotted lines outline the positions of the contact pads and the nanowire. The scale bar is 500 nm.

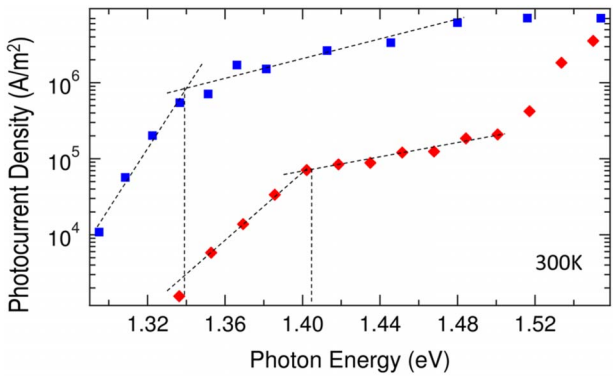

FIG. 3. (Color online) Photocurrent vs photon energy for a ZB (blue square symbols) and WZ (red diamond symbols) nanowire devices. A sharp change in slope is clearly seen corresponding to the nanowire band gap, as indicated by vertical dashed lines. A bias voltage of 5 V and an excitation power density of 30 W/cm^2 was used for all measurements.

devices, estimated to be ~0.5–0.6 μm in the dark, cannot be resolved given our laser spot size (diameter of ~0.8 μm).

To investigate the sensitivity of the photoresponse to the excitation wavelength, we defocus the laser so that the entire device is illuminated and scan the laser wavelength from 700 nm (well above the gap) to 1000 nm (well below the gap) and keep the bias voltage (5 V) and the power of the diffused laser fixed (30 W/cm^2). Figure 3 shows a comparison of wavelength-dependent photocurrent in WZ and ZB nanowire devices. As the laser wavelength is scanned from higher energies to close to the band edge, the photocurrent drops monotonically. A clear signature of the band gap can be seen as an abrupt change in the slope which occurs at 1.408 eV for the 20 nm, WZ nanowire and 1.338 eV for the 50 nm, ZB nanowire. Below these energies the photocurrent density exhibits the expected Urbach tail and drops exponentially by orders of magnitude until the induced current becomes smaller than the dark current.[13] We note that the slopes of the subgap photocurrent energy dependence in our data (Urbach parameters of 24 meV for ZB and 33 meV for WZ) are in reasonable agreement with the light absorption data for bulk InP, and most likely result from defects or phonons.[14] The larger Urbach parameter for the WZ nanowire may indicate the presence of more disorder. The observed 70 meV ($\pm$4 meV) difference between the threshold energies agrees well with the 80 meV shift between ZB and WZ InP nanowires as measured optically at low temperatures.[3,4,7,8] Strongly mixed ZB/WZ nanowires (not presented here) do not exhibit such well-defined changes in the slope.

We have shown that one can make single nanowire MSM nanodevices using photolithography which can distinguish WZ or ZB crystal structure even at room temperature. This technique is also sensitive to the presence of mixed phases or disorder and defects in the nanowire, and may be a rapid means for characterization of NW growths including measurements of their band gaps. Since these simple nanodevices are sensitive to incident light fluences as low as 8 nW, it appears possible to use lamp spectrographs which would enable measurements of UV or infrared materials (e.g., ZnO, GaN, or GaSb) where tunable laser sources are not readily available.

We acknowledge the support of the NSF through DMR Grant Nos. 0806700 and 0804199, and ECCS Grant No.

0701703, as well as the University of Cincinnati Institute for Nanoscale Science and Technology. The Australian authors acknowledge support from the Australian Research Council. The Australian National Fabrication Facility established under Australian government NCRIS program is acknowledged for access to the facilities used in this work.

[1]J. Appenzeller, J. Knoch, M. I. Bjork, H. Riel, H. Schmid, and W. Riess, IEEE Trans. Electron Devices **55**, 2827 (2008).
[2]J. M. Bao, D. C. Bell, F. Capasso, J. B. Wagner, T. Martensson, J. Tragardh, and L. Samuelson, Nano Lett. **8**, 836 (2008).
[3]A. Mishra, L. V. Titova, T. B. Hoang, H. E. Jackson, L. M. Smith, J. M. Yarrison-Rice, Y. Kim, H. J. Joyce, Q. Gao, H. H. Tan, and C. Jagadish, Appl. Phys. Lett. **91**, 263104 (2007).
[4]K. Pemasiri, M. Montazeri, R. Gass, L. M. Smith, H. E. Jackson, J. Yarrison-Rice, S. Paiman, Q. Gao, H. H. Tan, C. Jagadish, X. Zhang, and J. Zou, Nano Lett. **9**, 648 (2009).
[5]R. E. Algra, M. A. Verheijen, M. T. Borgstrom, L. F. Feiner, G. Immink, W. J. P. van Enckevort, E. Vlieg, and E. Bakkers, Nature (London) **456**, 369 (2008).
[6]P. Caroff, K. A. Dick, J. Johansson, M. E. Messing, K. Deppert, and L. Samuelson, Nat. Nanotechnol. **4**, 50 (2009).
[7]J. Tragardh, A. I. Persson, J. B. Wagner, D. Hessman, and L. Samuelson, J. Appl. Phys. **101**, 123701 (2007).
[8]M. Mattila, T. Hakkarainen, M. Mulot, and H. Lipsanen, Nanotechnology **17**, 1580 (2006).
[9]S. Paiman, Q. Gao, H. H. Tan, C. Jagadish, K. Pemasiri, M. Montazeri, H. E. Jackson, L. M. Smith, J. M. Yarrison-Rice, X. Zhang and J. Zou, Nanotechnology **20**, 225606 (2009).
[10]Z. Y. Zhang, K. Yao, Y. Liu, C. H. Jin, X. L. Liang, Q. Chen, and L. M. Peng, Adv. Funct. Mater. **17**, 2478 (2007).
[11]Y. Gu, E. S. Kwak, J. L. Lensch, J. E. Allen, T. W. Odom, and L. J. Lauhon, Appl. Phys. Lett. **87**, 043111 (2005).
[12]Y. Gu, J. P. Romankiewicz, J. K. David, J. L. Lensch, and L. J. Lauhon, Nano Lett. **6**, 948 (2006).
[13]M. Grundmann, *The Physics of Semiconductors: An Introduction Including Devices and Nanophysics* (Springer, Berlin, 2006).
[14]W. J. Turner, W. E. Reese, and G. D. Pettit, Phys. Rev. **136**, A1467 (1964).